Desalination and Water Treatment
www.deswater.com

doi: 10.5004/dwt.2021.27828

241 (2021) 171–182
November

Applying iron coating on the Saudi Arabia volcanic tuff for enhancing mercury adsorption from synthetic wastewater

Noureddine Elboughdiri[a,b,*], Djamel Ghernaout[a,c], Amari Abdelfattah[d,e], Muhammad Imran Khan[f], Alsamani Ahmed Salih[a], Mohammed Matouq[g]

[a]*Chemical Engineering Department, College of Engineering, University of Ha'il, P.O. Box 2440, Ha'il 81441, Saudi Arabia, Tel. +966549571015; email: ghilaninouri@yahoo.fr (N. Elboughdiri)*
[b]*Chemical Engineering Process Department, National School of Engineers Gabes, University of Gabes, Gabes 6011, Tunisia*
[c]*Chemical Engineering Department, Faculty of Engineering, University of Blida, P.O. Box: 270, Blida 09000, Algeria*
[d]*Department of Chemical Engineering, College of Engineering, King Khalid University, Abha 61411, Saudi Arabia*
[e]*Department of Chemical Engineering, Research Laboratory of Energy and Environment, National School of Engineers, Gabes University, Gabes 6072, Tunisia*
[f]*Research Institute of Sciences and Engineering, University of Sharjah, Sharjah, 27272, United Arab Emirates*
[g]*Al-Balqa Applied University, Chemical Engineering Department, Amman, P.O. Box: 4486, 11131 Jordan*

Received 31 December 2020; Accepted 21 September 2021

ABSTRACT

The collected volcanic tuff was modified and characterized using X-ray diffraction, scanning electron microscopy (SEM), and cation exchange capacity (CEC). The sorption behavior of two samples of volcanic tuff was determined by a set of parametric batch experiments that were conducted as a function of pH, ionic strength (I), and the concentration of selected metals. The particle characterization revealed that iron oxide coating was successfully applied onto the surface of volcanic tuff and showed high CEC (1.02 mol/kg for the natural Kingdom of Saudi Arabia (KSA) volcanic tuff and 0.81 mol/kg for the modified volcanic tuff), specific surface area, and uniform distribution of iron. The SEM illustrated that the concentration of iron varied between the different spectra. The CEC of the modified volcanic tuff decreased relative to their nature and was proportional to the concentration of iron used in the modification process. Applying iron-coating increased the mercury removal capacity of the KSA volcanic tuff up to 100%, specifically at the higher initial concentration (IC) of Hg (8.76 mg/L) and low I (0.01 M $NaNO_3$). In contrast, for low IC of Hg (0.0876 mg/L) and high I (1 M $NaNO_3$), the experiments did not indicate an increase in the sorption process efficiency. More experiments with a wider range of pH values, silicate, sulfate, carbonate, and ionic strength are needed to fully quantify the dependence of maximum sorption on such factors.

Keywords: Adsorption; Ion exchange; Mercury (Hg); Volcanic tuff; Sorption; Wastewater

1. Introduction

The geographic location of the Kingdom of Saudi Arabia (KSA) gives its area to have good natural solid resources that are rich in minerals having unique physicochemical properties. These minerals can be used in different engineering and industrial applications. Volcanic tuff is used in wastewater treatment to remove harmful pollutants. This method of treatment is based on its cation-exchange behavior, thus making this sorbent limited to cation removal. As an example, a large amount of volcanic tuff is found in KSA especially at Jabal Salma and Al Harrah Al Birk, an area in the

---

* Corresponding author.

North West of the country. Several research studies were performed to determine the possibility of using volcanic tuff in different engineering applications such as a material of construction, a raw material in the cement industry, a lightweight aggregate, and an adsorbent for removing various types of environmental pollutants from wastewater [1–4]. Tremendous work was done to develop good technologies to reduce heavy metals and, thus, a feasible low-cost technology is needed to achieve the desired results [5–9]. The dominant technologies that are available for removing heavy metals from wastewaters include electrodialysis, membrane processes (e.g., reverse osmosis, ultrafiltration), chemical precipitation, adsorption and ion exchange [4–6]. According to the literature review, there is a very little and limited number of researches that have been performed on local KSA volcanic tuff for its potential usage in environmental and industrial applications [1–3,8]. Recently, volcanic tuff minerals have been used in wastewater treatment as ion exchangers for removing hazardous pollutants including radioactive cations (Sr^{2+}, Cs^{+}) and heavy metals (Cu^{2+}, Pb^{2+}, and Cd^{2+}). This technology depends on the cation exchange behavior in which the dissolved cations from wastewater are exchanged with cations on volcanic tuff exchange sites [1–3]. Iron oxides have a high adsorption capacity for removing several pollutants from wastewater. This is thanks to their characteristics such as high surface area, surface charge, and high affinity towards metals and metalloids. However, when iron oxides are used by themselves, they become difficult to remove from the water after adsorption and, therefore, need to be placed as a coating onto particles to give them some mechanical stability [6,7]. volcanic tuffs with iron oxide coating showed to be a good sorption media for absorbing harmful contaminants from wastewater such as heavy metals and polyphenols.

The natural properties, such as high surface area and cation exchange capacity (CEC), give good advantages to modified volcanic tuffs. In addition, more advantages are related to the adsorption properties of iron oxides such as great attraction sites for contaminants retention [10–12]. This work aims to characterize this mineral by determining its chemical composition and physical properties as well as evaluating its potential use to remove the mercury that has harmful effects from contaminated wastewater.

2. Materials and methods

2.1. Volcanic tuff samples

To study the natural volcanic tuff, three different samples were collected from different places and characterized using different techniques. Scanning electron microscopy (SEM) showed that most particles in the volcanic tuff are present as an anhedral mass with rare crystal faces or edges. The X-ray diffraction (XRD) analysis confirmed that anhedral masses contained the clinoptilolite. The Brunauer–Emmett–Teller surface area analysis showed that volcanic tuff had high surface area and high CEC. Trace element analysis indicated that significant concentrations of mercury (189 ppm) were naturally present in the volcanic tuff. This result must be taken into account regarding batch sorption experiments. The main composition of the three samples are presented in Table 1.

2.2. Coating methods

To study the possibility of removing mercury from wastewater by adsorption, a crashed volcanic tuff was prepared in the laboratory and then was coated with iron oxide following the same technique previously published [18–22]. In such a technique, an iron oxide-coated medium is prepared by treating 0.67–0.99 mm volcanic tuff with 0.5 M ferric nitrate. The sorption was assessed in batch tests and the sample was reported to be an effective sorbent for metal ions. The SEM analysis revealed that the principal elements of the dried coated volcanic tuff were Fe and Si. Before use, the tuff was pretreated with HCl acid solution (pH = 1, 2 M) for 24 h, rinsed with deionized water, and dried at 100°C for 24 h. A concentrated stock solution of 2 M Fe(III) was prepared by adding ultrapure water to 160.8 g of $Fe(NO_3)$ in a 200 mL flask. The stock solution was stored in a labeled polypropylene bottle. Thereafter, a stock solution of 0.5 M was prepared by dissolving a more

Table 1
Characteristics of the KSA volcanic tuff [13–17]

	Sample #1#	Sample #2#	Sample #3#	Average	Standard deviation
SiO_2 (%)	42.1	39.3	37.5	38.4	2.3
TiO_2 (%)	2.5	2.7	2.6	2.6	0.1
Al_2O_3 (%)	9.9	9.3	10.0	9.7	0.4
Fe_2O_3 (%)	11.1	11.4	11.7	11.4	0.3
MnO (%)	0.2	0.2	0.2	0.2	0.0
MgO (%)	9.3	9.1	8.4	8.9	0.5
CaO (%)	10.3	10.7	10.4	10.5	0.2
Na_2O_3 (%)	2.3	2.9	2.6	2.6	0.3
K_2O (%)	3.2	3.7	3.0	3.3	0.4
LOI[a] (%)	9.1	10.0	13.0	10.7	2.0
SUM (%)	100.1	99.3	99.3	99.6	0.5

[a] LOI: Loss on ignition.

concentrated solution, and sodium hydroxide was added to the mixture until a pH = 9.5 was reached followed by continued mixing for about 15 min.

25 mL of the stock solution was added to the tuff and the mixture was placed in a drying oven at 50°C for 4 d. Finally, the coated tuff was washed with deionized water and dried at 100°C overnight; and, then, it was stored for further use.

2.3. Batch experiments

Mercury sorption has been reported to be significantly affected by pH and ionic strength (I). This is explained by the fact that these factors affect the competition of the ions present in the solution with the ions of interest for sorption sites. In addition, it was shown that the greater I the lower the sorption uptake of mercury [23,24]. Other studies showed that a negative correlation could exist between initial metal concentration and fractional sorption uptake [14,24]. The mineralogy of the particles, the combination of ions of interest, and the initial concentration (IC) of interest metal suggested that the equilibration time in this study would differ from the previously conducted studies [19–21].

The experiments were performed as a function of time, pH, I, and initial metal concentration at a constant temperature (25°C). The solution of Hg is prepared with high purity by dissolving 0.1354 g of mercuric chloride in 75 mL of reagent water, adding 10 mL of concentrated nitric acid, and adjusting the volume to 100 mL. All chemicals used were of analytical grade supplied by Karl Fischer® with purity >99%. All vessels and instruments were cleaned by soaking in detergent solution, then acid bath and in deionized water for at least 24 h.

The levels of the key variables along with the experimental design are represented in Table 2. The experiments were duplicated, and each set of samples included a control blank solution.

Samples were dried, sieved through a 0.25 mm sieve, and stored in a desiccator. After that, the tuff was introduced into 250 mL polypropylene bottles, the metal of interest was added to the reactors, and the timer was started. At different times, an amount of the sample was collected, filtered using 0.25 mm syringe filters. The filtrate was collected into test tubes, the supernatant was controlled, and the pH was adjusted if needed with 70% HNO_3. The analysis of the residual mercury was conducted at the SGS Laboratories (Tunisia) using graphite furnace Atomic Absorption Spectrometry.

Table 2
Summary of the range and levels of the key selected variables

Variable	Number	Values/Types
Type of sorbent	2	KSA volcanic tuff and modified volcanic tuff
Type of sorbate	1	Mercury (Hg)
Sorbate initial concentration (IC)	2	IC = 0.0876 and IC = 8.76 mg/L
Ionic strength (I)	2	I = 0.01 M $NaNO_3$ and I = 1 M $NaNO_3$
pH	3	4, 7, and 9
Sampling times (t)	5	1, 60, 120, 180, and 240 h

3. Results and discussion

3.1. Sample characterization

The sorption process depends on particle properties such as porosity, specific surface area, pore size distribution, morphology, and CEC. Therefore, these properties should be examined to correctly evaluate the sorption potential of the two types of volcanic tuffs. The uniformity of iron oxide coating and the effect of the iron concentration on the modified surfaces were examined to confirm that coating application was successful [14–17].

3.1.1. Particle morphology

SEM images have high special resolution and a large depth of field [25,26]. They are used in geological applications for imaging and are useful for judging the surface structure and for examination of the surface characteristics of the sample. In this project, photomicrography of the exterior surface was obtained by SEM (Keysight Technologies, U9320A 8500) and images were taken at 1,000×. Distribution and intensity were determined by comparing the images of coated and uncoated volcanic tuff, accompanied by energy-dispersive X-ray (EDS) readings (Tables 3 and 4).

Table 3
Composition of the KSA volcanic tuff

Test	O (%)	Al (%)	Si (%)	K (%)	Fe (%)
1	46.51	5.03	40.85	4.21	0
2	33.99	7.35	50.75	5.17	0
3	51.04	4.92	38.04	2.67	0
Mean	43.85	5.77	43.21	4.02	0
Standard deviation	8.83	1.37	6.68	1.26	0

Table 4
Composition of the modified volcanic tuff

Test	O (%)	Si (%)	K (%)	Fe (%)
1	50.85	20.30	2.49	23.51
2	55.83	10.09	1.14	2.01
3	21.67	38.45	15.84	24.04
Mean	42.78	22.95	6.49	16.52
Standard deviation	18.45	14.36	8.12	11.03

The major elements of the natural volcanic tuff are silicon, oxygen, aluminum, and potassium, while iron was not detected. The iron content of the tuff modified with 0.5 M ferric nitrate ranged from 2% to 24%, with an average of 13% (Table 4). The modified tuff has a high amount of iron while the raw has no iron content due to the Coating Method used.

Fig. 1 reveals that the modified volcanic tuff surfaces are evidently occupied by iron oxide. Such a modification was formed during the coating process.

The compositional spectra for coated modified samples showed uniform distribution of the iron on the surface. These results were obtained for three different areas on the sample surface. In addition, the spectra revealed the absence of iron in the KSA volcanic tuff (Table 3).

The compositional trends are further evident in the color modification of volcanic tuff in response to iron coating, which changed from light gray to yellow. According to the diagnostic criteria of iron oxide minerals, samples with red coloring indicate the presence of hematite, and samples with brown-red and yellow coloring indicate the presence of goethite. Furthermore, the color intensity is proportional to the amount of iron oxide applied onto volcanic tuff: natural volcanic tuff (SVT) (none) < modified volcanic tuff (MVT) (SVT treated with 0.5 M ferric nitrate).

3.1.2. Mineral composition

The presence of the minerals within the adsorbent and to know the form of iron on the surface of coated particles can be investigated by using the XRD technique. In this study, the mineralogic and crystallographic analysis of the volcanic tuff was determined using XRD (Thermo Scientific, ARLTM X'TRA) at the SGS Laboratories (Tunisia). Before the analysis, the samples were dried overnight in the oven at 100°C and stored in the desiccator to prevent hydration of the samples. The obtained results are presented in Figs. 2 and 3.

The KSA volcanic tuff is composed primarily of clinoptilolite (36%) and feldspar (64%). However, the spectra of modified volcanic tuff contained a peak in iron corresponding to the formation of hematite (9%) during the coating process at high temperatures. These results are consistent with those of previous studies, which reported the formation of hematite on the surface of modified volcanic tuff [22–26].

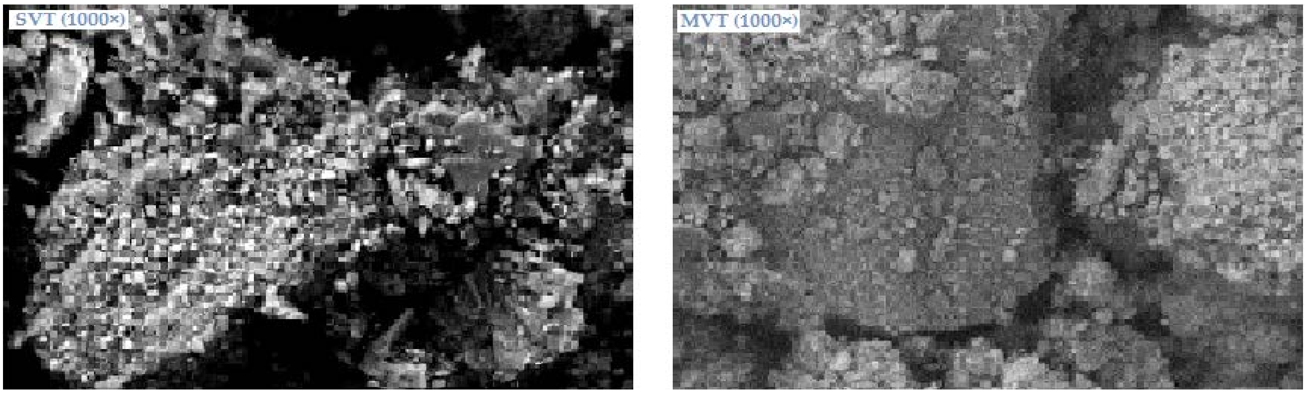

Fig. 1. Scanning electron microscopy (SEM) micrographs of natural volcanic tuff (SVT) and coated volcanic tuff (MVT), 1,000 × magnification.

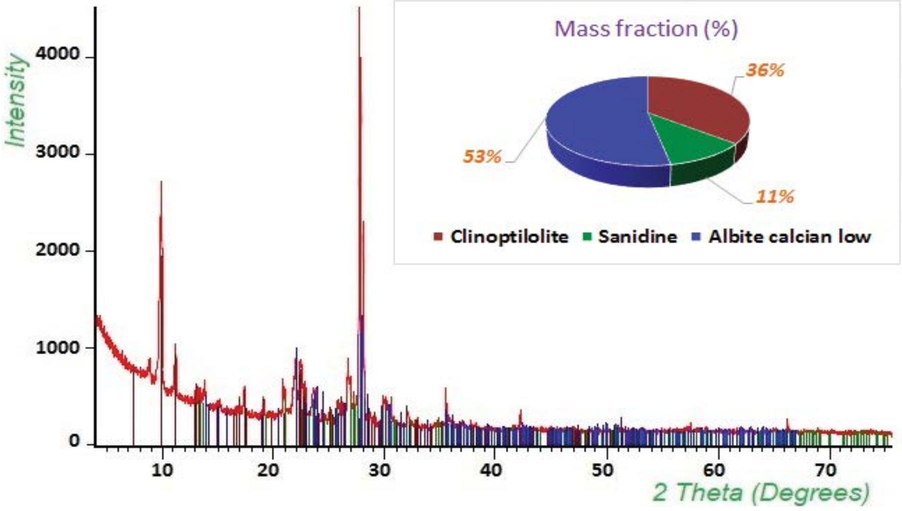

Fig. 2. The X-ray diffraction (XRD) of the KSA volcanic tuff.

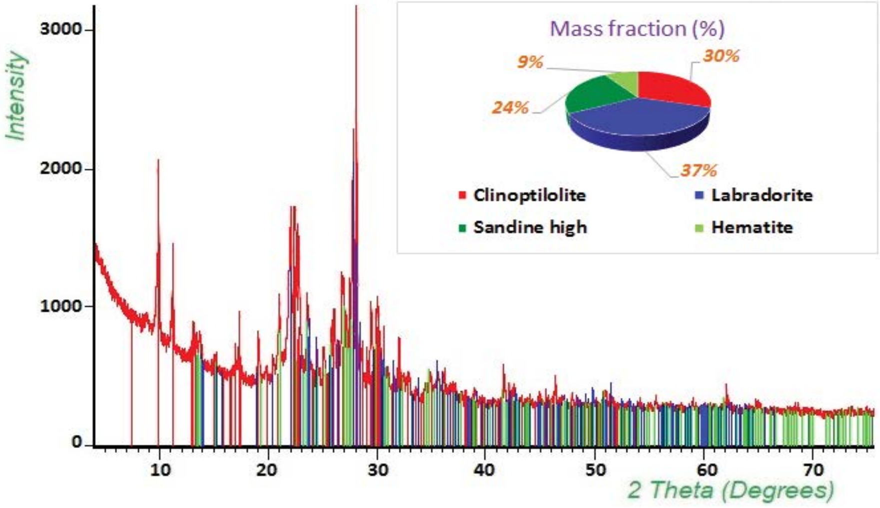

Fig. 3. The X-ray diffraction (XRD) of the modified volcanic tuff.

3.1.3. Cation exchange capacity

The ability of a mineral to exchange one type of cation with another is called CEC. This property is a measure of the quantity of the readily exchangeable cations per unit weight neutralizing negative charge and is commonly expressed in moles per kg (mol/kg). The different procedures of the measurements method, as well as the condition of the experiments, can affect the CEC results [1,14–16]. Therefore, in the present study, the determination of CEC was performed at the SGS Laboratories (Tunisia) using a method employed by Burt [27]. According to this method, the exchange sites were saturated with an index cation (NH_4^+) by leaching the samples using 1N NH_4OAc and a vacuum extractor. The extract was weighed and saved for analysis. Then, ethanol was used to rinse NH_4^+ saturated samples to remove the fraction not adsorbed. The sample was then rinsed with 2M KCl, and the leachate was analyzed calorimetrically to determine the adsorbed amount of NH_4^+ [28–30]. The analysis was performed in duplicates and the average was reported as CEC equal to 1.02 mol/kg for the natural KSA volcanic tuff and 0.81 mol/kg for the modified volcanic tuff. For the same experimental conditions, the CEC found in the literature is 1.39 mol/kg [15–19]. The decrease in CEC values is proportional to the concentration of iron applied onto tuff: SVT (none) < MVT (with 0.5 M ferric nitrate). Linking SEM to the EDS results, it can be said that iron oxide mineral growth effectively reduced the number of cation-exchange sites. The obtained results were compared to those of previous studies performed by Alsawalha et al. [17], where the CEC of natural volcanic tuff for the same particle size was reported to be 1.40 mol/kg.

3.2. Sorption uptake of mercury

In order to evaluate the mercury removal capacity of the modified volcanic tuff, batch experiments were performed as a function of deferent parameters; time, *I*, acidity, and initial metal concentration. The difference between the initial and the final metal concentrations in the supernatant was used to determine the sorption uptake. It is expressed as a percentage of the original metal concentration. Before the calculation, all concentrations were adjusted according to corrected blanks and calculated based on the average of duplicates experiments.

The residual metal ions of Hg at time *t* (q_t, mg/g) were calculated using the following equation [31].

$$q_t = \frac{(C_i - C_t)V}{m} \times 100 \tag{1}$$

where C_i and C_t are is the initial concentration (mg/L) and the residual concentration at time *t* (mg/L) respectively, *V* is the volume of industrial wastewater (L) and *m* is the weight of adsorbent (g).

3.2.1. Effect of time

Fig. 4 shows the sorption of mercury as a function of time for KSA tuff and modified volcanic tuff at a low IC of Hg (0.0876 mg/L) and higher *I* (1 M). The residual concentration dropped below the limit detection of the instrument (0.03 mg/L) showing maximum sorption of more than 40% for the two samples. The concentrations increased over the experiment, suggesting that mercury was leached from the volcanic tuff.

Fig. 5 illustrates that at a higher IC of Hg (8.76 mg/L) and low I (0.01 M) the maximum sorption of 100% was reached within 120 h. However, at high I (1 M), there was very little to no sorption throughout the experiment as presented in Fig. 6.

3.2.2. Effects of ionic strength (I) and pH

Batch sorption experiments with two *I* (0.01 M $NaNO_3$ and 1 M $NaNO_3$) are performed to demonstrate the iron coating effect on the removal of mercury from wastewater. Figs. 7 and 8 show that the sorption behavior for the two types of volcanic tuffs at both ICs and low I appears to be

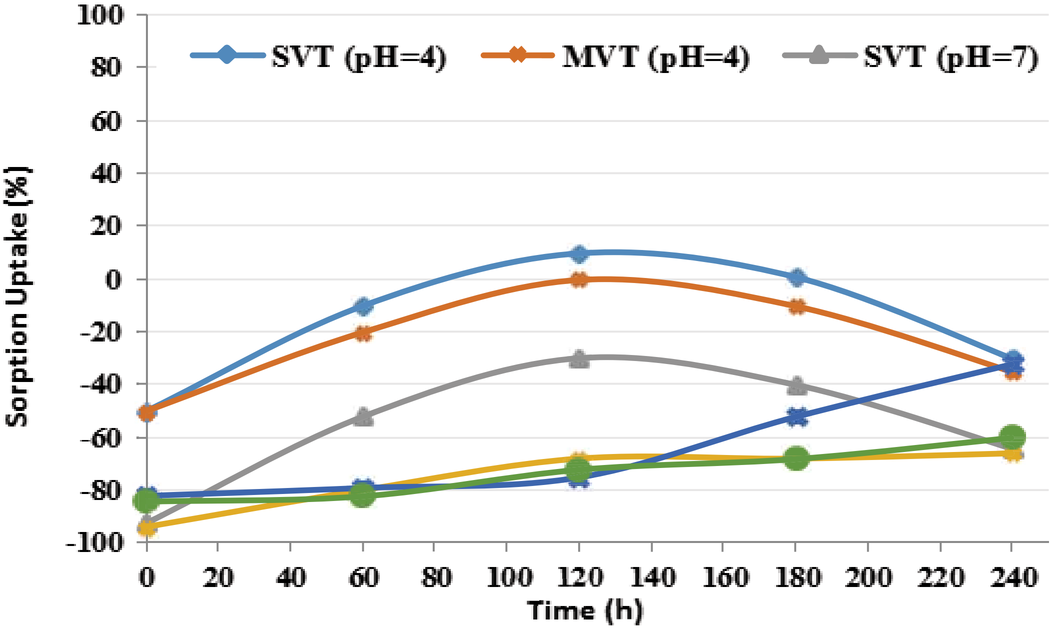

Fig. 4. Sorption of Hg as a function of time for KSA volcanic tuff (SVT) and modified volcanic tuff (MVT), IC = 0.0876 mg/L, *I* = 1 M $NaNO_3$.

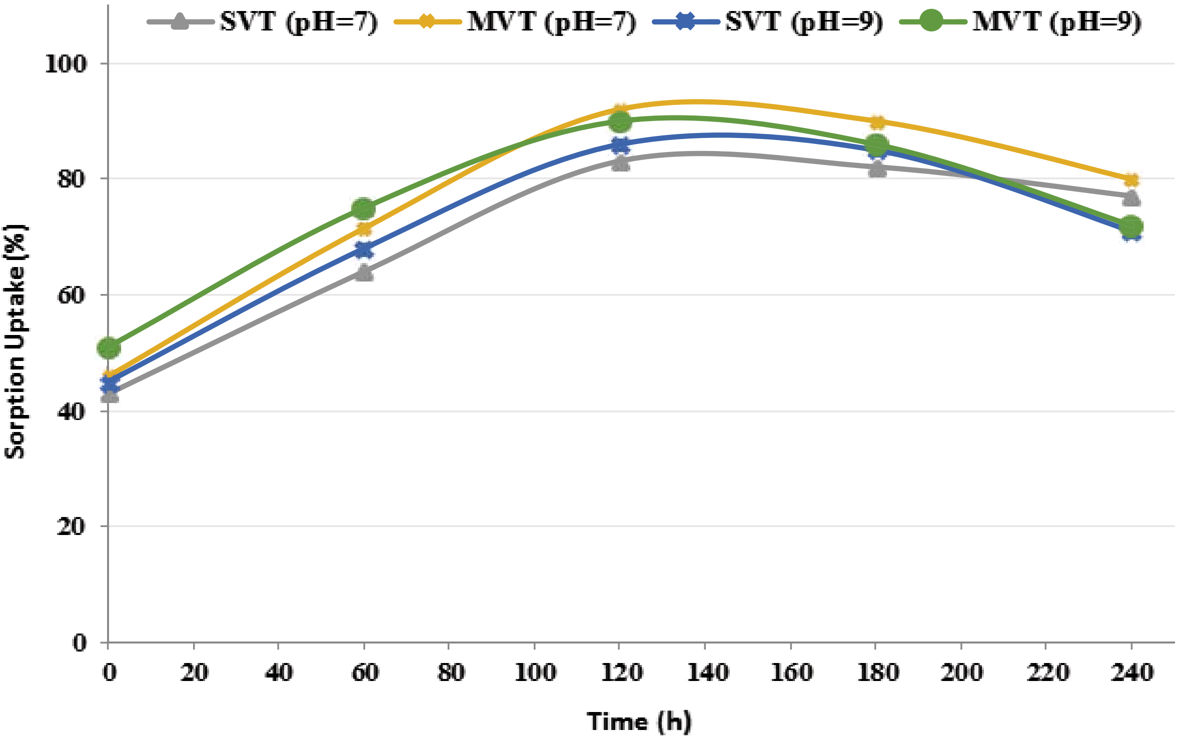

Fig. 5. Sorption of Hg as a function of time for KSA volcanic tuff (SVT) and modified volcanic tuff (MVT), IC = 8.76 mg/L, *I* = 0.01 M $NaNO_3$.

pH-independent. This may suggest that despite modification, the sorption of Hg ions is highly dependent on the concentration of competing electrolyte ions due to the nature of complexes formed by Hg and the volcanic tuff.

Fig. 7 shows that at a higher IC of Hg (8.76 mg/L) and low *I* (0.01 M $NaNO_3$) both modified and KSA tuffs removed up to 100% of Hg from the wastewater. However, at higher *I* (1 M $NaNO_3$) both sorbents showed no sorption due to

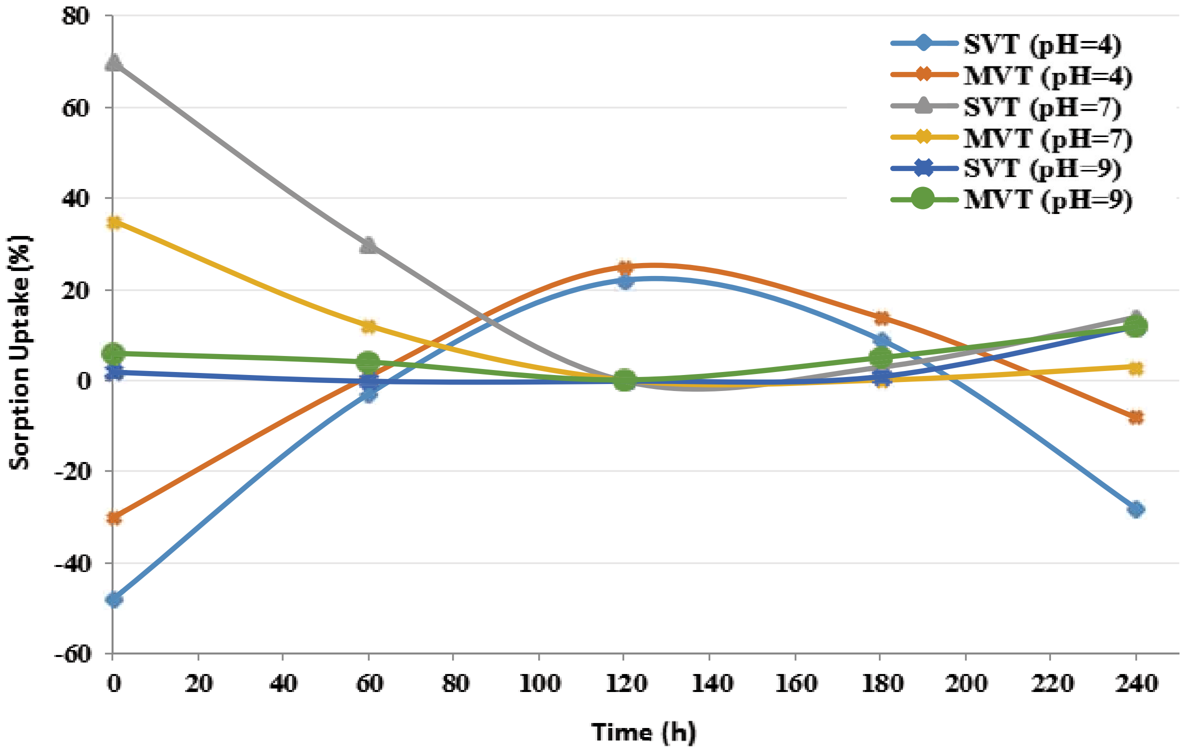

Fig. 6. Sorption of Hg as a function of time for KSA volcanic tuff (SVT) and modified volcanic tuff (MVT), IC = 8.76 mg/L, *I* = 1 M $NaNO_3$.

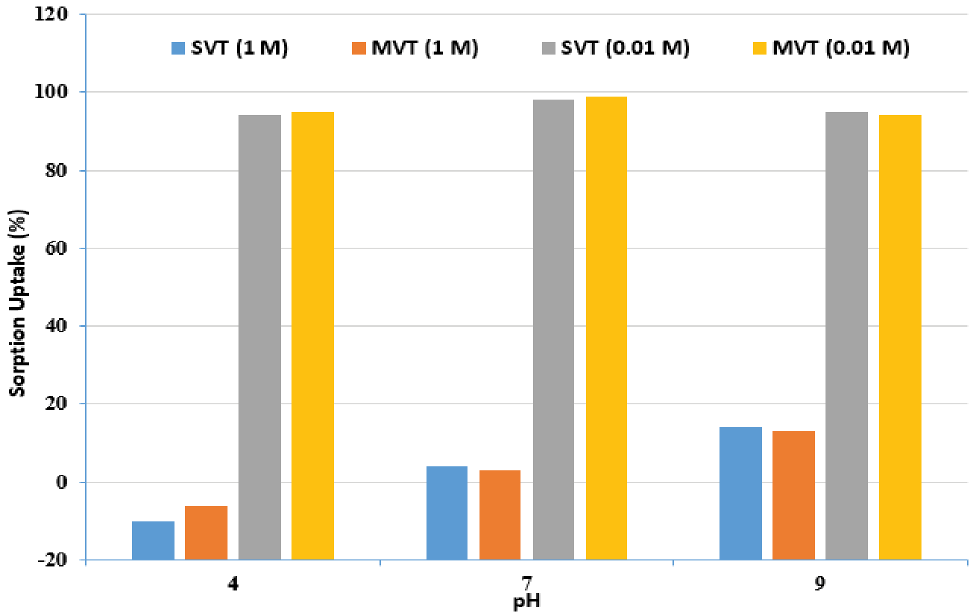

Fig. 7. Sorption of Hg as a function of pH for KSA volcanic tuff (SVT) and modified volcanic tuff (MVT), IC = 8.76 mg/L.

the competition of mercury with sodium ions. As *I* was increased by the addition of sodium nitrate ($NaNO_3$), the number of sodium ions increased, thus more effectively competing with mercury ions.

The interaction between the cations and the surface can be chemically by sharing electrons or physically through the Van der Waals forces. Therefore, cations can associate with a surface by forming internal or external complexes depending on whether a cation forms a chemical bond with an electron-donating oxygen ion on the surface or a cation of opposite charge approaches the surface group within a critical distance. External complexes require

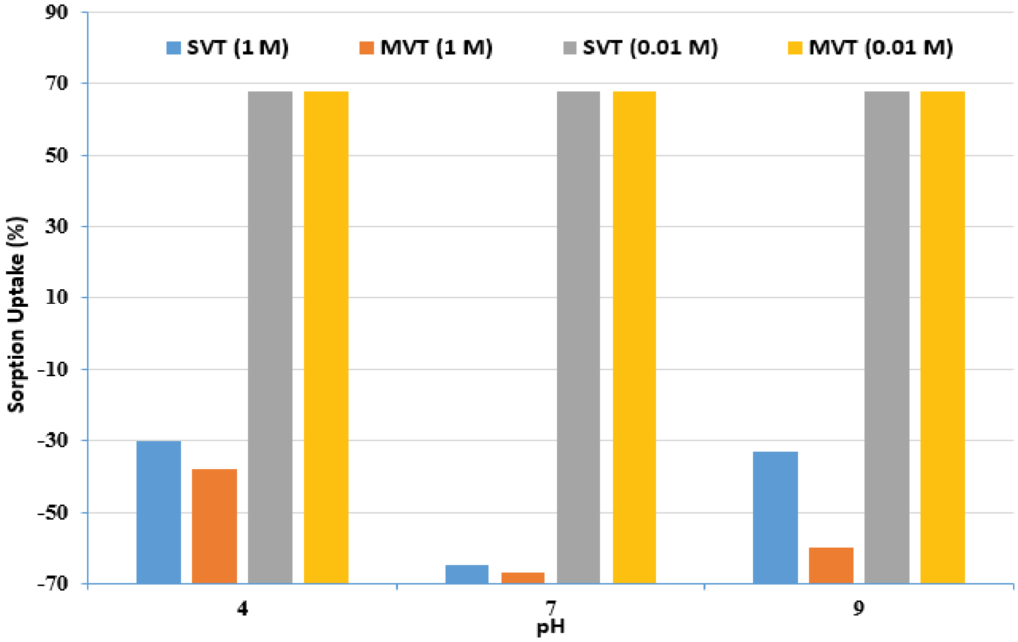

Fig. 8. Sorption of Hg as a function of pH for KSA volcanic tuff (SVT) and modified volcanic tuff (MVT), IC = 0.0876 mg/L.

electrostatic bonding mechanisms and therefore are weaker than internal complexes. The dependence of sorption on the concentration of electrolyte suggests that Hg forms external complexes with the surface groups of volcanic tuffs [18–21].

The sorption of mercury into the modified volcanic tuff with iron can be explained as a result due to sorption of Hg ions onto Fe-sites with the formation of internal complexes and the competition between mercury with sodium in the surface iron coated [17–19].

3.2.3. Effect of initial metal concentration

Several publications indicate that a decrease in the concentration of Hg should increase the fractional sorption uptake [6–8]. However, the results obtained in this study did not reveal this trend. In fact, experiments performed at low *I* (0.01 M) and low IC of Hg (0.0876 mg/L) revealed negative sorption, indicating that there was actually more Hg in the solution that was added at the beginning of the experiment. KSA volcanic tuff contains about 189 mg/kg of Hg, suggesting that prior to injection the reactors contained up to 0.14 mg. Increasing the IC of Hg over the course of batch experiments suggests that ions naturally occurring in volcanic tuff were exchanged with sodium ions present in the solution.

Fig. 9 illustrates that at low *I* (0.01 M) and high IC of Hg (8.76 mg/L), the sorption behavior is similar for both types of volcanic tuffs and exhibit sorption close to 0%. The analysis of the filtrate with low *I* and low concentration of Hg (IC = 0.0876 mg/L) revealed that Hg ion concentration was below the detection limit of 0.03 mg/L, resulting in fractional sorption uptake of at least 66%. Previous studies, with the same concentration and similar initial metal concentration (2.5 mg/L), reported fractional sorption uptake greater than 95% [22–24].

The obtained results for high *I* (1M $NaNO_3$) are presented in Fig. 10. The experiments did not indicate an increase in the sorption efficiency with low IC (0.0876 mg/L) and show sorption uptakes of 100% for high IC of Hg (8.76 mg/L).

3.3. Sorption isotherm models

Several isotherm models are available to describe this equilibrium sorption distribution. Two of these isotherm equations were adopted in this study.

The Langmuir sorption isotherm is used to estimate the maximum adsorption capacity corresponding to complete monolayer coverage on the adsorbent surface and is expressed by the following linearized form [31]:

$$\frac{1}{q_e} = \frac{1}{\left(q_{\max} K_L C_e\right)} + \frac{1}{q_{\max}} \tag{2}$$

where q_e is the amount of adsorbate adsorbed per unit weight of adsorbent (mg/g), C_e is the equilibrium concentration in mg/l, K_L (L/mg) is a constant related to the adsorption/ desorption energy and $q_{\max}$ is the maximum sorption upon complete saturation of the biomass surface (mg/g).

The Freundlich sorption isotherm is one of the most widely used mathematical descriptions and gives an expression encompassing the surface heterogeneity and the exponential distribution of active sites and their energies. The linearized form of the Freundlich isotherm is [31]:

$$\log q_e = \log K_F + \frac{1}{n} \log C_e \tag{3}$$

where q_e is the amount of adsorbate adsorbed per unit weight of adsorbent (mg/g), C_e is the equilibrium concentration in

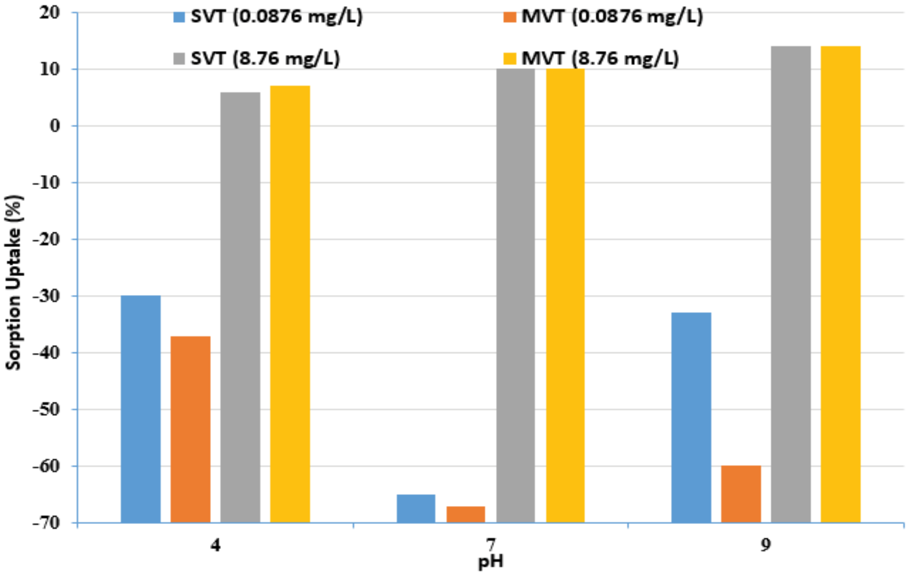

Fig. 9. Sorption of Hg as a function of metal concentration for KSA volcanic tuff (SVT) and modified volcanic tuff (MVT), *I* = 0.01 M as $NaNO_3$.

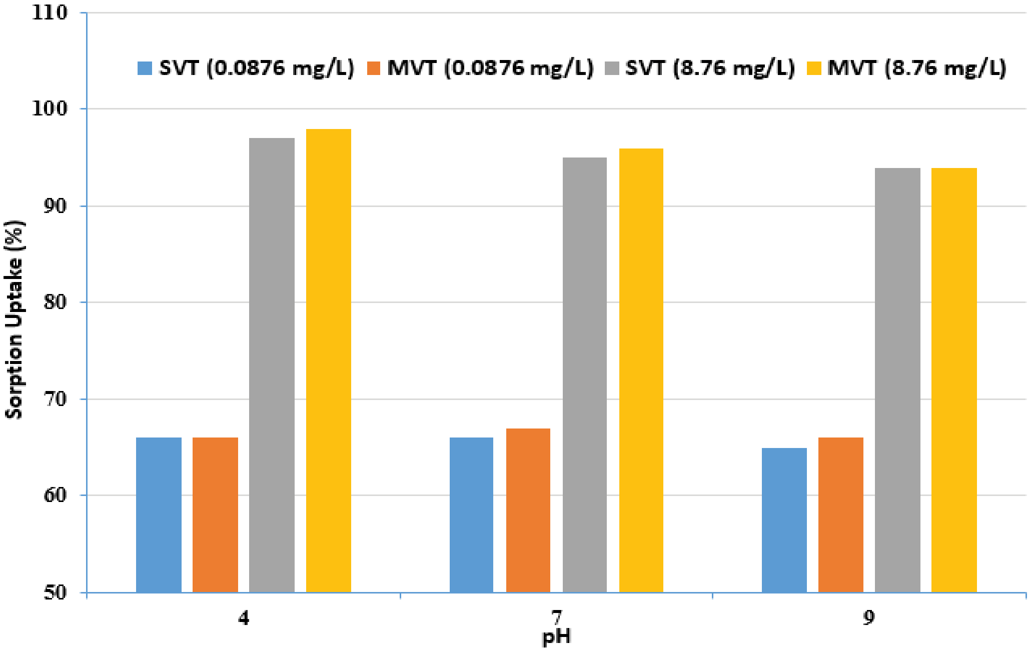

Fig. 10. Sorption of Hg as a function of metal concentration for KSA volcanic tuff (SVT) and modified volcanic tuff (MVT), *I* = 1 M as $NaNO_3$.

mg/l, K_F is a parameter related to the temperature (mg/g $(L/mg)^{1/n}$), and "n" is a characteristic constant for the adsorption process.

The experimental data is then fitted into the above equations for linearization by plotting $1/q_e$ and $\log q_e$ against C_e. After each adsorption, the residual metal ions of Hg at time t (q_t, mg/g) were calculated using Eq. (1).

Six mixed solutions with concentrations 25, 50, 75, 100, 150 and 150 mg/L of Hg are made by proper dilution of stock solution. The pH was adjusted and maintained at 7 throughout the experiment. 25 mL of the prepared samples were poured into six flasks. 10 g of the adsorbent was introduced to each flask and was agitated. Thereafter the concentrations of Hg were determined, the equilibrium data obtained from this experiment were observed to fit with Langmuir and Freundlich isotherm models.

Plotting $1/q_e$ against $1/C_e$ for both types of volcanic tuff as shown in Fig. 11 indicates that the equilibrium data

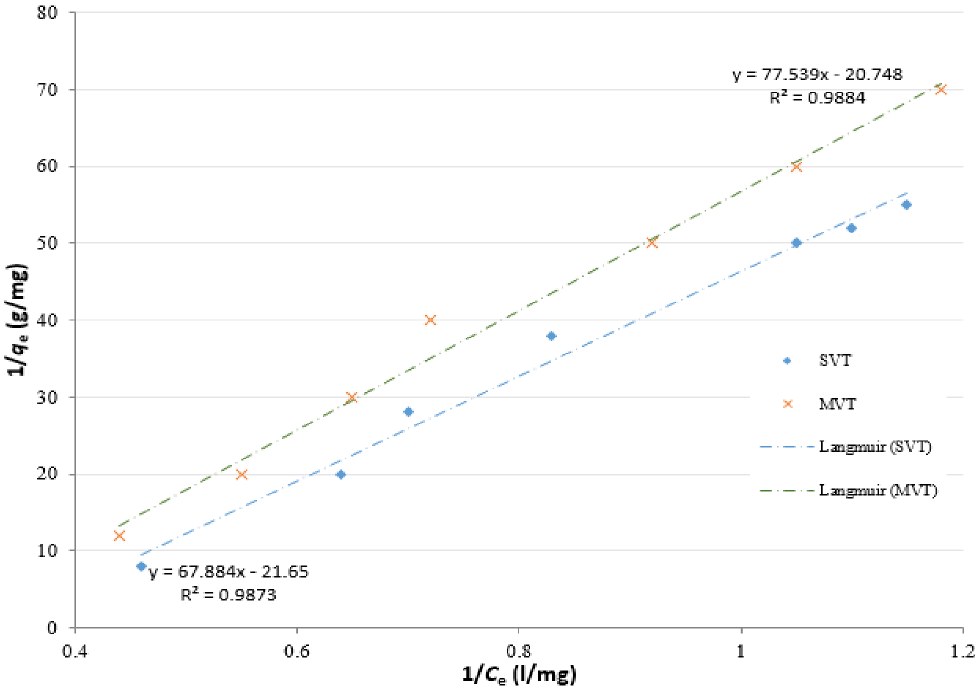

Fig. 11. Removal of mercury ions (Hg^{2+}) by natural volcanic tuff (SVT) and modified volcanic tuff (MVT) fitted to Langmuir isotherm.

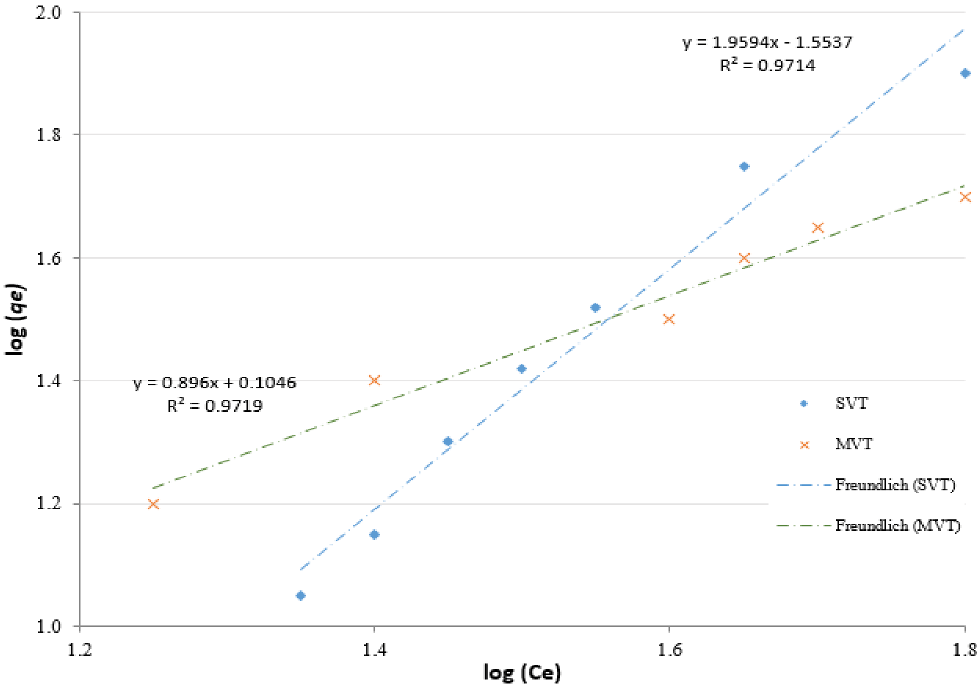

Fig. 12. Removal of mercury ions (Hg^{2+}) by natural volcanic tuff (SVT) and modified volcanic tuff (MVT) fitted to Freundlich isotherm.

follows the Langmuir model. The correlation between $\log q_e$ and $\log C_e$ is presented in Fig. 12 and the adsorption of mercury ions onto the adsorbents gave a straight line indicates good adsorption and that the equilibrium data follows the Freundlich model.

Langmuir and Freundlich parameters and correlation coefficient square R^2 are presented in Table 5, showing that the experimental data deviate more in the case of the Freundlich model than the Langmuir model for the studied adsorbents. The removal of Hg by SVT and MVT is better described by the Langmuir isotherm.

Table 5
Freundlich and Langmuir isotherm constants for adsorption of mercury from synthetic wastewater using natural volcanic tuff (SVT) and modified volcanic tuff (MVT)

	Isotherm parameters	Natural volcanic tuff (SVT)	Modified volcanic tuff (MVT)
Langmuir	Equation	$y = 67.884x–21.65$	$y = 77.539x–20.748$
	R^2	0.9873	0.9884
	$q_{\max}$ (mg/g)	64.58	69.15
	K_L (L/mg)	6.7	5.2
Freundlich	Equation	$y = 1.9594x–1.5537$	$y = 0.896x + 0.1046$
	R^2	0.9714	0.9719
	n	0.99	0.99
	K_F (mg/g (L/mg)$^{1/n}$)	0.57	0.65

4. Conclusion

In this study, the natural and modified volcanic tuffs were characterized by determining particle size, CEC, specific surface area, particle mineralogy, and the distribution of the coating of iron oxide.

Particle characterization revealed that iron oxide coating was successfully applied onto the surface of volcanic tuff and showed high CEC, specific surface area, and uniform distribution of iron. The SEM showed that iron oxide coating was distributed throughout the surface in clusters and the concentration of iron varied between the different spectra. CEC of the modified volcanic tuff decreased relatively to natural volcanic tuff and was proportional to the concentration of iron used in the modification process.

The sorption capacity of the two samples of volcanic tuff was determined by a set of parametric batch experiments, which were performed as a function of pH, I, and the concentration of selected metals.

Sorption studies revealed that the application of iron-coating increased the mercury removal capacity of KSA volcanic tuff up to 100%, specifically in the higher IC of Hg (8.76 mg/L) and low I (0.01 M $NaNO_3$). In contrast, for low IC of Hg (0.0876 mg/L) and high I (1 M $NaNO_3$), the experiments did not indicate an increase in the sorption process.

Further investigation is needed to evaluate the competition between cations and anions for sorption sites on iron oxide-coated volcanic tuff. Additional batch experiments with a wider range of pH values, silicate, sulfate, carbonate, and ionic strength are needed to fully quantify the dependence of maximum sorption on these variables and to understand the competitive on Hg removal by iron-coated volcanic tuff.

Acknowledgments

This research has been funded by the Research Deanship of the University of Ha'il, Saudi Arabia, through Project RG-20 113.

Conflicts of interest

The authors declare that they have no known competing financial interests or personal relationships that could have appeared to influence the work reported in this paper.

References

[1] A. Ababneh, F. Matalkah, Potential use of Jordanian volcanic tuffs as supplementary cementitious materials, Case Stud. Constr. Mater., 8 (2018) 193–202.

[2] N. Elboughdiri, The use of natural zeolite to remove heavy metals Cu(II), Pb(II) and Cd(II), from industrial wastewater, Cogent Eng., 7 (2020) 1–13.

[3] K.K. Al-Zboon, J.A. Al-Tabbal, N.M. Al-Kharabsheh, N.K. Al-Mefleh, Natural volcanic tuff as a soil mulching: effect on plant growth and soil chemistry under water stress, Appl. Water Sci., 9 (2019) 123, doi: 10.1007/s13201-019-1000-2.

[4] M. Dines, V.K. Gupta, S.K. Srivastava, S. Chander, Kinetics of mercury adsorption from wastewater using activated carbon derived from fertilizer waste, Colloids Surf., A, 177 (2001) 169–181.

[5] K.B. Payne, T.M. Abdel-Fattah, Adsorption of divalent lead ions by zeolites and activated carbon: effects of pH, temperature, and ionic strength, J. Environ. Sci. Health. Part A Toxic/Hazard. Subst. Environ. Eng., 39 (2004) 2275–2291.

[6] B. Kozera-Sucharda, B. Gworek, I. Kondzielski, The simultaneous removal of zinc and cadmium from multicomponent aqueous solutions by their sorption onto selected natural and synthetic zeolites, Minerals, 10 (2020) 343, doi: 10.3390/min10040343.

[7] R.Y. Wu, Y. Wang, X.Y. Xue, T.P. Hu, J.F. Gao, F.Q. An, Selective adsorption and removal ability of pine needle-based activated carbon towards Al(III) from La(III), J. Dispersion Sci. Technol., 40 (2019) 186–191.

[8] K.K. Al-Zboon, B.M. Al-Smadi, S. Al-Khawaldh, Natural volcanic tuff-based geopolymer for Zn removal: adsorption isotherm, kinetic, and thermodynamic study, Water Air Soil Pollut., 227 (2016) 248, doi: 10.1007/s11270-016-2937-5.

[9] R. Menhaje-Bena, H. Kazemian, S. Shahtaheri, M. Ghazi-Khansari, M. Hosseini, Evaluation of iron modified zeolites for removal of arsenic from drinking water, Stud. Surf. Sci. Catal., 154 (2004) 1892–1899.

[10] N. Mojoudi, N. Mirghaffari, M. Soleimani, H. Shariatmadari, C. Belver, J. Bedia, Phenol adsorption on high microporous activated carbons prepared from oily sludge: equilibrium, kinetic and thermodynamic studies, Sci. Rep., 9 (2019) 19352, doi: 10.1038/s41598-019-55794-4.

[11] Y. Taamneh, S. Sharadqah, The removal of heavy metals from aqueous solution using natural Jordanian zeolite, Appl. Water Sci., 7 (2017) 2021–2028.

[12] M. Malihe, S. Parastar, M. Mahdavi, A. Ebrahimi, Evaluation efficiency of Iranian natural zeolites and synthetic resin to removal of lead ions from aqueous solutions, Appl. Water Sci., 10 (2020) 60, doi: 10.1007/s13201-019-1135-1.

[13] J.C. Hsu, C.J. Lin, C.H. Liao, S.T. Chen, Removal of As(V) and As(III) by reclaimed iron-oxide coated sands, J. Hazard. Mater., 153 (2008) 817–826.

[14] M. Al-Anbar, Z. Al-Anbar, Utilization of natural zeolite as ion-exchange and sorbent material in the removal of iron(III), Desalination, 225 (2008) 70–81.

[15] M. El Hajam, N.K. Idrissi, G.-I. Plavan, H. Abdel Halim, L. Mansour, F. Boufahja, A. Zerouale, Pb^{2+} ions adsorption onto raw and chemically activated Dibetou sawdust: application of experimental designs, J. King Saud Univ. – Sci., 32 (2020) 2176–2189.

[16] K. He, Y. Chen, Z. Tang, Y. Hu, Removal of heavy metal ions from aqueous solution by zeolite synthesized from fly ash, Environ. Sci. Pollut. Res., 3 (2016) 2778–2788.

[17] M. Alsawalha, Overview of current and future perspectives of Saudi Arabian Natural Clinoptilolite Zeolite: a case review, J. Chem., 2019 (2019) 3153471, doi: 10.1155/2019/3153471.

[18] N. Elboughdiri, Effect of time, solvent-solid ratio, ethanol concentration and temperature on extraction yield of phenolic compounds from olive leaves, Eng. Technol. Appl. Sci. Res., 8 (2018) 2805–2808.

[19] E. Aboud, N. El-Masry, A. Qaddah, F. Alqahtani, M.R.H. Moufti, Magnetic and gravity data analysis of Rahat Volcanic Field, El-Madinah city, Saudi Arabia, NRIAG J. Astron. Geophys., 4 (2015) 154–162.

[20] S.F. Lütke, A.V. Igansi, L. Pegoraro, G.L. Dotto, L.A.A. Pinto, T.R.S. Cadaval Jr., Preparation of activated carbon from black wattle bark waste and its application for phenol adsorption, J. Environ. Chem. Eng., 7 (2019) 103396, doi: 10.1016/j.jece.2019.103396.

[21] S. Rekha, R. Sapna, N. Manjula, K. Dinesh, Kinetics and adsorption studies of mercury and lead by ceria nanoparticles entrapped in tamarind powder, ACS Omega, 3 (2018) 14606–14619.

[22] A.S. Nizami, O.K.M. Ouda, M. Rehan, A.M.O. El-Maghraby, J. Gardy, A. Hassanpour, S. Kumar, I.M.I. Ismail, The potential of Saudi Arabian natural zeolites in energy recovery technologies, Energy, 108 (2016) 162–171.

[23] M. Visa, N. Popa, Adsorption of heavy metals cations onto zeolite material from aqueous solution, J. Membr. Sci. Technol., 5 (2015) 133.

[24] U.T. Mehmet, A.A. Mehmet, Possibility of using Kütahya Volcanic Tuff as building stone: microstructural evaluation and strength enhancement through heat treatment, Constr. Build. Mater., 110 (2016) 128–134.

[25] M.M. Sakineh, N.E. Alireza, Supported iron oxide onto an Iranian clinoptilolite as a heterogeneous catalyst for photodegradation of furfural in a wastewater sample, Desal. Water Treat., 57 (2016) 10802–10814.

[26] G. Garcia, E. Cardenasa, S. Cabrera, J. Hedlund, J. Mouzon, Synthesis of zeolite Y from diatomite as silica source, Microporous Mesoporous Mater., 219 (2019) 29–37.

[27] R. Burt, Soil Survey Laboratory Methods Manual, United States Department of Agriculture, 2004, pp. 173–180.

[28] R.P. Han, L.N. Zou, X. Zhao, Y.F. Xu, F. Xu, Y.L. Li, Y. Wang, Characterization and properties of iron oxide-coated zeolite as adsorbent for removal of copper(II) from solution in fixed bed column, Chem. Eng. J., 149 (2009) 123–131.

[29] P. Belousov, A. Semenkova, T. Egorova, A. Romanchuk, S. Zakusin, O. Dorzhieva, E. Tyupina, Y. Izosimova, I. Tolpeshta, M. Chernov, V. Krupskaya, Cesium sorption and desorption on glauconite, gentonite, zeolite, and diatomite, Minerals, 9–10 (2019) 625, doi: 10.3390/min9100625.

[30] M.R. Hassan Moufti, K. Nemeth, The Intra-Continental Al Madinah Volcanic Field, Western Saudi Arabia: A Proposal to Establish Harrat Al Madinah as the First Volcanic Geopark in the Kingdom of Saudi Arabia, Geoheritage, 5 (2013) 185–206.

[31] N. Elboughdiri, Olive mill wastewater phenolic compounds adsorption onto active olive stones: equilibrium isotherms and kinetics study, Int. J. Forensic Eng., 4 (2018) 31–46.